



HAL
open science

Coordination Adaptable Networks: Introducing Vitrimer Properties Using Dynamic Coordination Bonds

Meenu Murali, Eric Manoury, Rinaldo Poli

► **To cite this version:**

Meenu Murali, Eric Manoury, Rinaldo Poli. Coordination Adaptable Networks: Introducing Vitrimer Properties Using Dynamic Coordination Bonds. *European Journal of Inorganic Chemistry*, 2023, 26 (36), pp.e202300574. 10.1002/ejic.202300574 . hal-04269901

HAL Id: hal-04269901

<https://hal.science/hal-04269901>

Submitted on 3 Nov 2023

HAL is a multi-disciplinary open access archive for the deposit and dissemination of scientific research documents, whether they are published or not. The documents may come from teaching and research institutions in France or abroad, or from public or private research centers.

L'archive ouverte pluridisciplinaire **HAL**, est destinée au dépôt et à la diffusion de documents scientifiques de niveau recherche, publiés ou non, émanant des établissements d'enseignement et de recherche français ou étrangers, des laboratoires publics ou privés.

Coordination Adaptable Networks: Introducing Vitrimers Properties Using Dynamic Coordination Bonds

Meenu Murali,^[a] Eric Manoury,^[a] and Rinaldo Poli*^[a]

[a] Dr. M. Murali, Dr. E. Manoury, Prof. R. Poli
 CNRS, LCC (Laboratoire de Chimie de Coordination)
 Université de Toulouse, UPS, INPT
 205 Route de Narbonne, BP 44099, F-31077, Toulouse Cedex 4, France
 E-mail: Rinaldo.poli@lcc-toulouse.fr

Abstract: Coordination adaptable networks (CooANs) may be obtained by combination of ligand-functionalized polymers and metal ions or clusters when the crosslink migration by ligand exchange with available free ligands in the polymer matrix is facile. These materials may be called “coordination vitrimers” if proven to follow an associative ligand exchange mechanism. The present review presents various types of CooANs, classified according to the nature of the metal-binding functions, e.g. imine, imidazoles, pyridines as L-type ligands; catecholates, thiolates, carboxylates as X-type ligands. Particular attention is placed on the crosslink migration mechanism.

1. Introduction

Thermoset polymers, given their unique mechanical properties and structural stability, have become a vital component in modern society. The multitude of benefits notwithstanding, thermosets present a growing problem of accumulation of non-degradable waste. This is due to the difficulty in recycling, given the static crosslinks in the 3D networks. On the other hand, thermoplastics can be melted and dissolved in appropriate solvents, hence be reprocessed, due to the weak cohesive Van der Waals interactions between the linear chains. However, they have poor mechanical properties compared to thermosets. In recent times, the advantages of these two large families of materials have been combined by the development of adaptable polymer networks (APNs),^[1] in which the crosslinks are activated with respect to degenerate exchange reactions by a stimulus, e.g. heat, light irradiation, or a pH or solvent change. The introduction of dynamic crosslinks provides the network with properties such as self-healing, reshaping, stress relaxation and shape memory, and make the material reprocessable and recyclable.

The types of dynamic crosslink in APNs can be classified into two families depending on the strength of the interaction: covalent and non-covalent (hydrogen bonding, π - π stacking, host guest interactions, ionic interactions, and metal coordination). The APN family with covalent crosslinks is also widely known as “covalent adaptable networks” (CANs). APNs can also be classified according to the mechanism of crosslink migration, which may be associative or dissociative. While non-covalent APNs, because of the low-strength interactions, generally undergo crosslink migration according to a dissociative mechanism, CANs may reshape on the basis of either a dissociative or an associative mechanism. In APNs characterized by a dissociative crosslink exchange, a loss of network integrity occurs upon application of



Meenu Murali obtained her BSc (2018) and MSc (2019) in Materials from the Indian Institute of Science (Bangalore). Subsequently, she joined the Prof. Navakanta Bhat group at the Centre for Nanoscience and Engineering (CenSE), IISc, as project intern where she worked on 2D MOF-based chemoresistive gas sensors. She has obtained a Ph.D. degree from the Université Paul Sabatier in 2023, under the co-supervision of Dr. Eric Manoury and Prof. Rinaldo Poli at the Laboratoire de Chimie de Coordination in Toulouse. Her research involved developing coordination vitrimers based on carboxylate ligand exchange that are reprocessable at low temperatures.

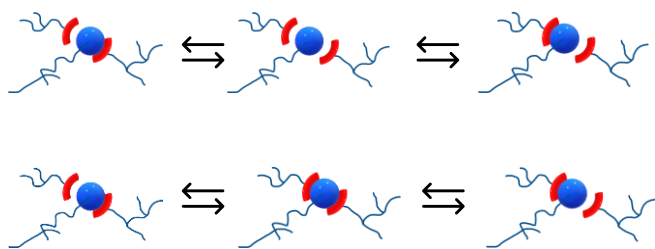


Eric Manoury graduated from the “Ecole Normale Supérieure de Cachan”. After a PhD in Orsay (G.G.A. Balavoine) on chiral perborates for alkene asymmetric epoxidation and a post-doc at MIT (B. Sharpless) on alkene asymmetric hydroxylation, he joined CNRS in 1993 in Orsay. He is currently First Class CNRS Research Director at the LCC Toulouse. Since 2010, he is coleader of the team “Ligands, Complex Architectures and Catalysis” in the LCC. Since 2018, he is LCC Deputy Director. His main research interests are: ferrocene chemistry, chiral ligand development, asymmetric catalysis including hydrogenations, oxidations and C-C coupling reactions, aqueous biphasic catalysis with polymeric nanoreactors, controlled radical polymerization.



Rinaldo Poli is Professor at the INP Toulouse since 2005, after holding positions at the University of Maryland, College Park and at the Université de Bourgogne, Dijon. He received several awards from the USA, France, Italy and Germany. Among his most recent recognitions, he was named Chemistry Europe Fellow in 2018, was inducted into the European Academy of Sciences in 2018, and received the Berthelot Medal (French Academy of Sciences) in 2020 and the Achille Le Bel award (French Chemical Society) in 2023. His research interests span several aspects of transition-metal chemistry: open-shell organometallics, spin-crossover reactivity, mechanistic studies, homogeneous catalysis, aqueous organometallic chemistry and biphasic catalysis, metal-mediated radical polymerization, coordination vitrimers.

the stimulus (Scheme 1A). Conversely, APNs characterized by an associative exchange maintain a constant crosslink density (Scheme 1B). In dissociative networks, the strength of the interaction crucially determines the dynamic properties, whereas in associative ones, rapid reshaping is possible even for strong bonds if the activation barrier is sufficiently low.



Scheme 1. Mechanism of crosslink exchange in adaptable polymer networks: A) dissociative; B) associative.

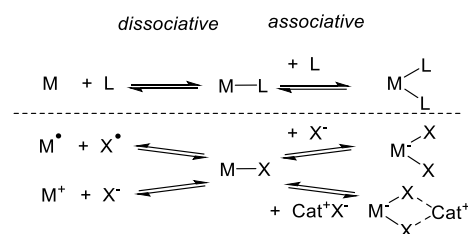
While the initially developed adaptable networks relied on dissociative exchange processes, namely stimulus-induced depolymerization-repolymerization, for either non-covalent^[2] or covalent^[3] crosslinks, interest then turned to associative exchange networks. After initial studies on photoactivated associative exchange processes based on radical chemistry,^[4] thermally activated, associative covalent networks were introduced in 2011 and named “vitrimers”, because they exhibit a rheological behavior qualitatively similar to that of vitreous silica.^[5] The first vitrimers were based on transesterification, but others based on a diversified range of exchange reactions were then developed, including disulfide exchange, imine exchange, transalkylation, *etc.*^[6] The viscosity decrease of vitrimers at high temperatures follows the Arrhenius law, although this property was shown to also extend to certain dissociative networks.^[7]

Of greater interest to the inorganic chemistry community, it is also possible to fabricate materials with dynamic properties based on the exchange of coordinative bonds. Metals ions or clusters have high and variable coordination numbers and can bind to a host of ligands than can easily be incorporated into organic linkers, rendering them ideal as crosslinkers in a 3D-network. In addition, ligand exchange reactions may occur through a mechanistic continuum from dissociative *via* interchange to associative, and extensive literature is available on the preferred mechanism as a function of metal and ligand nature. We can thus name these materials “Coordination Adaptable Networks” (CooANs), though they were initially referred to as “self-healing metallopolymers”. In case the exchange process is proven to be associative, the materials may be named “coordination vitrimers”. Either flexible multifunctional ligands or ligand-functionalized polymers may be conceived as organic matrix to embed the metal crosslinks. Since the degenerative exchange of coordination bonds generally proceeds with lower activation barrier relative to the degenerative exchange of covalent bonds, the reshaping of CooANs can generally be expected to occur under milder conditions than that of CANs.

Using metal ions or clusters as crosslinkers in 3D-materials is also commonplace in the large family of metal-organic frameworks (MOFs), in which these crosslinkers (called “structural building units” or SBU, in the jargon of that trade) are connected by multifunctional ligands (called “linkers” or “struts”), which are generally rigid, not allowing facile reshaping.^[8] The topology, hence the chemistry, of CooANs is thus equivalent to that of MOFs, except that the organic linker must be flexible to allow the crosslink migration by exchange of the coordinative bonds. MOFs can therefore be a great source of inspiration for the fabrication of CooANs, but Nature has also been a source of inspiration, as many biological materials able to reshape thanks to the action of metals ions are known, as will be pointed out in a

few examples below. Contrary to MOFs, CooANs do not have a well-defined 3D structure and have very low porosity for gas absorption, but can be swollen by liquids to an extent that depends on the strength of the matrix-liquid interactions and on the degree of crosslinking. Thus, CooANs with hydrophilic matrices can easily be swollen by water (hydrogels), whereas those with hydrophobic matrices are swollen by organic solvents. Rigid but still reshapable materials are accessible by increasing the crosslink density or by lowering the organic linker flexibility (*e.g.* higher glass transition temperatures).

In addition to self-healing and reshaping, interest in CooANs is justified by the additional properties linked to the nature of the metal centers, such as magnetism, dielectrics, luminescence and catalysis. After the first examples,^[9] which appeared at the same time as the first organic vitrimers, self-healing metallopolymers have developed very rapidly and reviews of this field are available.^[10] However, these materials have not been systematically scrutinized in terms of the metal-ligand exchange mechanism, *i.e.* on their potential classification as “coordination vitrimers”.



Scheme 2. Possible exchange mechanisms for L-type and X-type ligands.

In the present article, we overview CooANs by focusing on the metal-ligand interaction and on the exchange mechanism. The review is organized by ligand type, distinguishing neutral (L-type) and anionic (X-type) donors. This distinction is useful, because an M-L bond is rather prone, especially for weak field ligands, to dissociation without charge separation, whereas the dissociation of an M-X bond entails either a rather energetically costly homolytic cleavage with formal metal reduction and generation of an X[•] radical, or a heterolytic cleavage to M⁺ and X⁻ with charge separation (Scheme 2), which should be unfavorable in a low-permittivity organic polymer matrix. The latter phenomenon, however, is less critical for polymers applied in an aqueous medium (*e.g.* hydrogels). On the other hand, an associative exchange process may be envisaged with metathesis of an accompanying cation (most often a proton in the conjugate acid HX).

2. Relevance of coordination chemistry

Most of the investigations on self-healing metallopolymers have focused on the materials properties (rheological, mechanical, thermal, self-healing aptitude) and much less attention has been devoted to the coordination chemistry of the crosslinking ion or cluster, let alone on the detailed mechanism (associative vs. dissociative) or the crosslink migration during reshaping. The nature of the counterion in the salt used for crosslinking is crucially important. As will be shown in specific examples below, the anion

effect on the mechanical and rheological properties has been clearly evidenced in several cases, but its specific role as a ligand, competing with the matrix coordinating groups, has rarely been considered. Other important aspects are the preferred coordination number and geometry of the metal ion or cluster used as crosslinkers, which are affected by the metal d^n configuration, spin state and ligand nature. Appreciation of these coordination chemistry properties can help in the formulation of reasonable hypotheses for the ligand exchange process. A final point that deserved close consideration is the permittivity of the medium in which the materials are synthesized and investigated, with specific relevance to the stabilization of charged species and their dissociation equilibria. When materials are synthesized and used in water, e.g. hydrogels, a coordinating anion such as chloride or acetate may well be replaced by a neutral ligand to afford a positively charged crosslink plus the free solvated anion. When the materials are produced in a low permittivity organic solvent or used as bulk/film, however, charge separation is not necessarily favored and depends on the anion coordinating power.

3. Neutral Ligands

The vast majority of the first developed CooANs were based on neutral ligands anchored on polymer matrices. This section will not be comprehensive and is only meant to provide a general overview of the type of ligands and metals used, *via* a few illustrative examples.

3.1. Imines

Imine functions have coordinative properties towards metal ions, but the imine exchange is also one of the organic reactions leading to covalent vitrimers based on the amine-aldehyde condensation in the presence of an excess of either one of the two reactive groups.^[11] In a recent contribution, the introduction of metal ions (5 mol % of Cu^{2+} , Mg^{2+} or Fe^{3+}) as the hydrated chloride salts in covalent polyimine vitrimers built by condensation of terephthalaldehyde (TPA), diethylenetriamine (DETA) and tris(2-aminoethyl)amine (TREN) (Figure 1) was reported to improve their creep, thermal and mechanical properties, as well as their resistance to solvent and acids, without affecting the network reprocessability. The Arrhenius activation energy (E_a) for stress relaxation is raised from 52.3 to 56.3 (Mg^{2+}), 67.7 (Cu^{2+}) and 107.3 (Fe^{3+}) kJ mol^{-1} .^[12] Thus, coordination to these metal ions only has a strengthening effect through an increase of the crosslink density. The coordination environment of the metal ions in the polymer matrix, presumably involving tridentate amine-diimine ligands, is unclear. It was only suggested by DFT calculations on molecular models, which did not consider chloride as a possible ligand, and the explicit implication of ligand exchange processes during the material reshaping, let alone their intimate mechanism, was not considered by these authors.

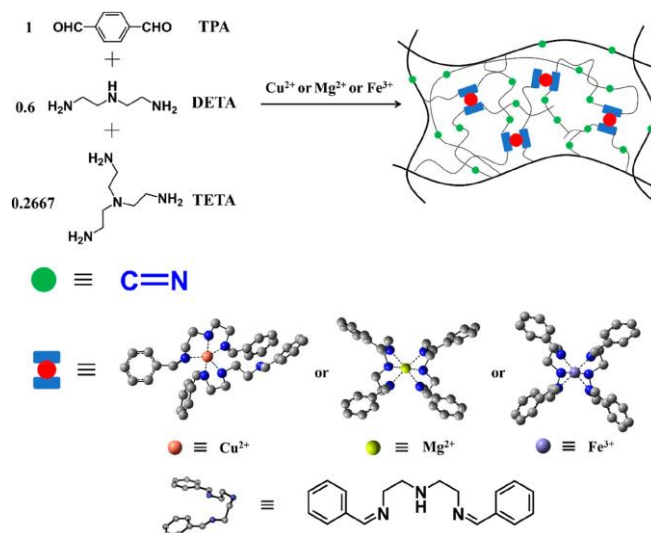


Figure 1. Synthetic route to metal ion-reinforced polyimine vitrimers. Reproduced with permission from ref. ^[12]. Copyright 2020 American Chemical Society.

Further studies on similar polyimine vitrimers, made from either isophthalaldehyde or 2,6-pyridinedicarboxaldehyde and the bio-based Priamine 1071 (Figure 2) addressed the impact not only of the cation (Mn^{2+} , Fe^{2+} , Co^{2+} , Ni^{2+} , Cu^{2+} , Zn^{2+}) but also of the corresponding anion (sulphate, nitrate, perchlorate, tetrafluoroborate, triflate and triflimide) and of the polymer-anchored ligand (iso-imine vs. pyr-imine) on the material properties (T_g , creep resistance, elastic modulus).^[13] The additional coordination bonds were shown to affect the imine exchange, in addition to increasing the crosslink density. The T_g and the elastic modulus (G') are correlated to the strength of the coordination bonds. However, once again, the direct implication of ligand exchange and the nature of its mechanism have not been addressed.

3.2. Imidazoles

Imidazoles are very common in Nature, notably in the histidine aminoacid, in biotin and in the imidazole alkaloids. The imidazole molecule is a relatively weak acid and typically binds to metal ions as an uncharged two-electron donor in neutral or acidic water, but can also lead to imidazolite complexes upon deprotonation at high pH.^[14] All examples of metallopolymers so far described exhibit imidazoles only as neutral donor. N-alkylated analogues are, of course, non-deprotonatable. The imidazole ring is generally linked to polymer chain *via* the ring 4 position, as in the histidine aminoacid, but linking *via* the 1 or 2 positions is also possible.

A number of self-healing polymeric materials based on metal-imidazole chemistry have been developed,^[15] inspired by the known biochemical role of zinc-histidine interactions in the high-toughness and self-healing properties of mussel byssal threads. When the imidazoles are not part of a chelating donor and the Zn^{2+} crosslinker is introduced as a salt with a non-coordinating anion, the nature of the crosslink is presumably $[\text{Zn}(\text{imidazole})_4]^{n+}$. An example of this situation is illustrated by the polystyrene-*graft*-poly(butyl acrylate) brushes made by RAFT polymerization (Figure 3), where imidazole is linked to the polymer chains *via* an N-linked tether and the metal bis(trifluoromethylsulfonyl)imide

(NTf₂) salt was used to crosslink.^[16] Additional work on these imidazole-functionalized polymer brushes, using NTf₂⁻ salts of Zn²⁺, Cu²⁺ and Co²⁺, correlated the mechanical properties to the preferred metal coordination geometry, to the ligand to metal ratio and to the ligand exchange mechanism of the imidazole-metal crosslinks.^[17] Different trends were observed, depending on the metal ion nature, for the mechanical properties as the L/M ratio is

changed. For Zn²⁺ and Cu²⁺, the viscosity and the extensibility remained unaltered until a sharp transition when L/M ≤ 4. On the other hand, the material based on Co²⁺ led to a gradual and proportional increase of the polymer solution and melt viscosity, as well as a decrease in extensibility. These results led the authors to propose an associative exchange for Zn²⁺ and Cu²⁺ and a dissociative one for Co²⁺ (Figure 4).

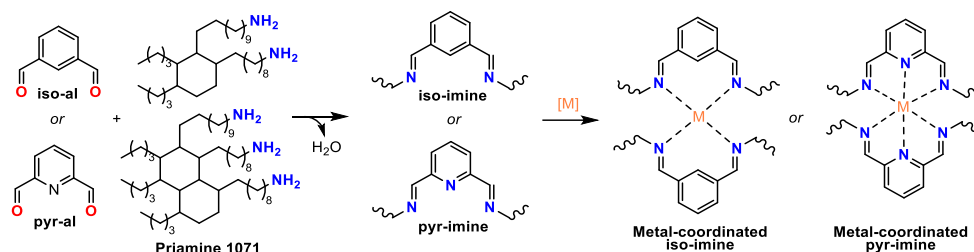


Figure 2. Reaction scheme for the synthesis of iso-imine and pyr-imine networks from reaction of either iso-al or pyr-al with Priamine 1071 (3:1 mixture of di- and triamine) and for the subsequent metal coordination.^[13]

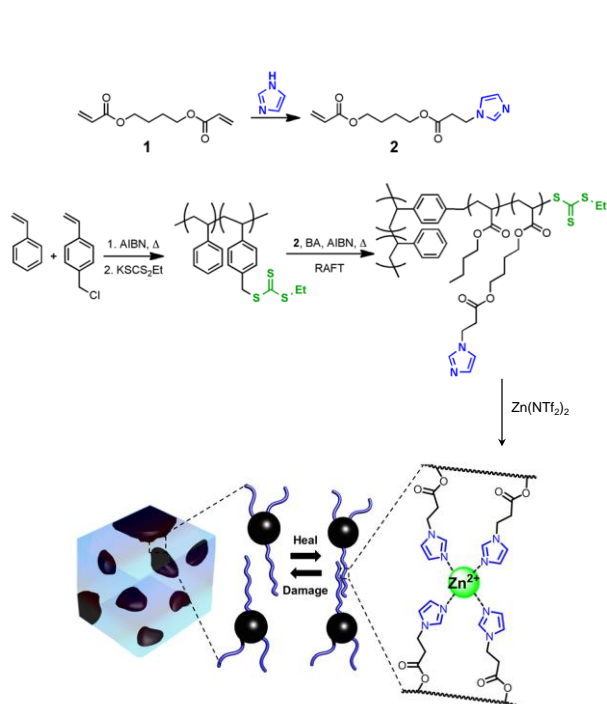


Figure 3. Synthesis of the imidazole-functionalized acrylate monomer and of the polystyrene-*graft*-poly(butyl acrylate) brush copolymer, crosslinking and self-healing process. Reproduced with permission from ref. ^[16]. Copyright 2014 American Chemical Society.

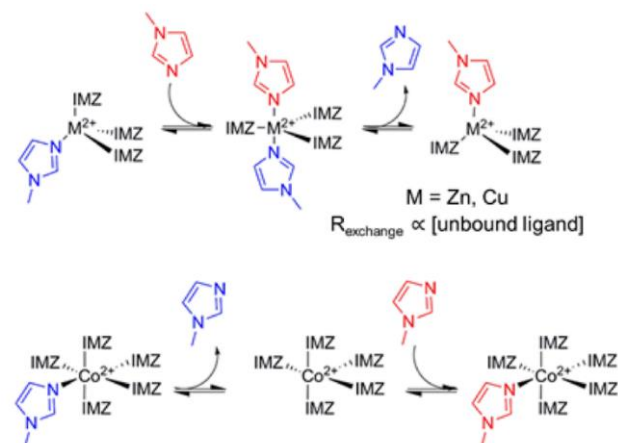


Figure 4. Different exchange mechanism for the crosslink migration in Adapted with permission from ref. ^[17]. Copyright 2016 American Chemical Society.

Another example of a material in which an imidazole group necessarily coordinates to the metal linker as a neutral ligand contains a methacrylamide comonomer (*N*^t-methacryloyl-*N*^t-tritylhistidine butyl amide), which is functionalized with an *N*-trityl-substituted imidazole linked to the polymerizable function *via* the ring 4 position (Figure 5). Symmetric ABA-type or BAB-type triblock copolymers differing in polymer architecture and molar mass, where the A block is polystyrene and the B block is a random copolymer of *n*-butyl acrylate and the histidine-functionalized acrylamide, were assembled by sequential RAFT (co)polymerization of the A and B (co)monomers, and then crosslinked by addition of different zinc salts (ZnCl₂ or Zn(OAc)₂).^[18] The high-temperature chain mobility during the healing process was assumed to result from “reversible cleavage” of the metal-ligand interactions, implying a dissociative process, which is in contrast with the conclusions made for the previous example (Figure 4).^[17] Indeed, Zn²⁺ is known to prefer tetra-coordination but is also commonly found as pentacoordinated and less frequently as hexacoordinated,^[19] and the interconversion of 4- and 5-coordinated Zn²⁺ complexes involving reversible

association of an imidazole ligand has been highlighted.^[20] Conversely, tricoordination for Zn^{2+} is quite rare and observed only in the presence of strong steric protection.^[21]

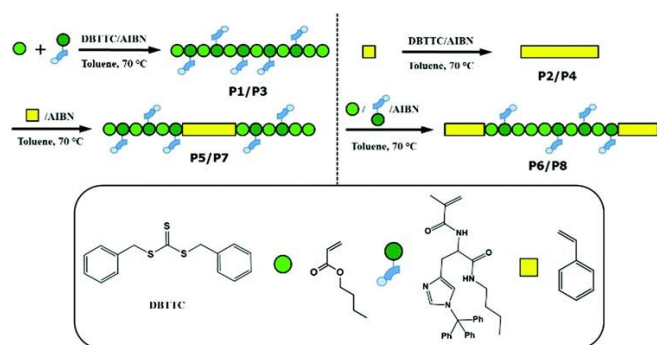
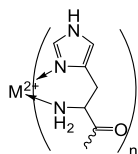


Figure 5. Synthesis of imidazole-functionalized triblock polymers by RAFT polymerization, for crosslinking by zinc salts. Reproduced with permission from ref. [18]. Copyright 2018 Royal Society of Chemistry.

A number of metallopolymers have also been generated with the non-substituted (1H) histidine, using Zn,^[22] Ni,^[22b, d, g, 23] Co,^[22b, 23d, 24] and Cu.^[22a, b, d, 23d] In these materials, the histidine coordination is generally proposed as bidentate *via* the imidazole N atom and the amine moiety (Scheme 1; e.g. $n = 2$ for Zn^{2+} , 2 or 3 for $Co^{2+/3+}$), but there is no solid evidence to support this assumption. Unfortunately, no X-ray structures are available for histidine-based complexes of these metals. Isothermal titration calorimetry^[22e, f] studies of the interaction between $ZnCl_2$ or $Zn(OAc)_2$ and various ligands in MeOH/ $CHCl_3$ (2:1) suggested ligand/metal ratios from 2 to 4, depending on the anion and ligand (molecular vs. polymer). Using the same ligand, $Zn(OAc)_2$ gave ligand/metal values *ca.* 1 unit greater than $ZnCl_2$, suggesting a competitive coordination of the chloride ion. Even if the salt counterions fully dissociate, however, the proposed^[22e] tetrakis-chelation (coordination number 8) appears quite unlikely. In brief, the coordination environment of the crosslinking metal ion in these materials is not well-established, and several readily interconvertible structures may be present at the same time.



Scheme 3. Chelating coordination mode most frequently invoked for histidine-based CooANs.

3.3. Pyridines

Pyridine ligands are widely used for metal bonding in polymers and are unambiguously neutral donors (L type). They are also often incorporated in multidentate chelating ligands (e.g. bipyridine, phenanthroline, terpyridine, etc.) to strengthen the binding affinity with metals. The first healable metallopolymer, described by Rowan *et al.* in 2011, is based on linear rubbery poly(ethylene-co-butylene) chains, end-functionalized with 2,6-bis(1'-methylbenzimidazolyl)pyridine ligands (Figure 6) and then crosslinked by addition of $Zn(NTf_2)_2$ or $La(NTf_2)_3$.^[9a] The La^{3+}

network was found more labile and more readily healable than the Zn^{2+} network. Healing could be promoted thermally or upon photoirradiation, the latter resting on photothermal conversion. The dynamics increased as the free ligand fraction increased, *i.e.* as x in $3 \cdot [Zn(NTf_2)_2]_x$ decreased from 1 to 0.7, which was interpreted as being linked to a viscosity decrease. Depolymerization was demonstrated at high temperatures, thus the ligand exchange process appears to have a dissociative character.

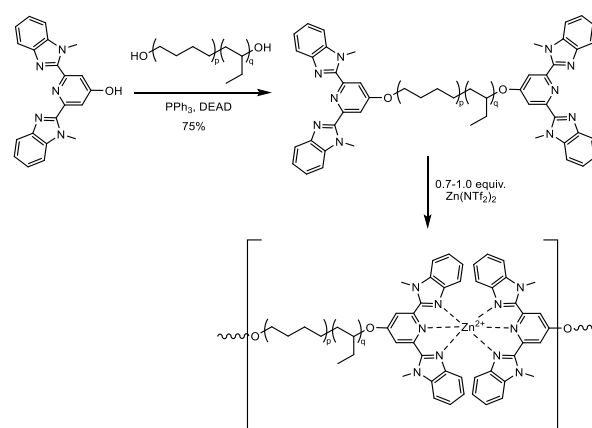


Figure 6. Synthesis of a chain-end 2,6-bis(1'-methylbenzimidazolyl)pyridine-functionalized macromonomer and polymerization by addition of $Zn(NTf_2)_2$ to yield a photohealable metallosupramolecular polymer. DEAD = diethyl azodicarboxylate.^[9a]

Related examples are linear polymethacrylates (methyl, butyl, lauryl), side-chain-functionalized with terpyridine ligands and crosslinked by addition of iron(II) sulfate, yielding quite stable $[Fe(terpy)_2]^{2+}$ crosslinks, which do not show any dissociation up to 100 °C.^[25] However, healing occurred at this temperature for the lower T_g polymers based on lauryl and butyl methacrylate. In the initial contribution, the authors proposed that the healing mechanism is related to the presence of ionic clusters, similar to the self-healing behavior of certain ionomers (e.g. Surlyn), hence not strictly related to the exchange of coordination bonds. This hypothesis was maintained in a later contribution, where the same polymer was crosslinked by different Cd^{II} salts.^[26] However, these investigations also revealed that the healing behavior depends on the nature of the counterion. The salts with more strongly binding anions (e.g. chloride, acetate) lead to faster healing, hinting to a possible contribution of ligand exchange processes. Indeed, a subsequent Raman investigation of these polymers, backed up by time-dependent DFT calculations, pointed to the probable partial decomplexation of the terpyridine ligands as the main contributor to the crosslink migration, facilitated by a non-innocent role of the anion.^[27] Further investigations on similar polymers, decorated by the same terpy ligand and crosslinked by a larger variety of metal salts, confirmed the crucial role of the metal-anion interaction for the healing process.^[28]

Another pyridine-based ligand used in metal-crosslinked networks is the bidentate pyridine-triazole. Linear polymers with a lauryl methacrylate backbone and side-chain-functionalized with these ligands were produced by RAFT polymerization, then crosslinked with various MA_2 salts ($M = Mn, Fe, Co$ and Cu ; $A = Cl, Br, OAc, OTf, BF_4$ or $A_2 = SO_4$). The materials exhibited good thermal healing performance, again dependent on the nature of

cation and counterion.^[29] As in many other similar contributions, the metal coordination was represented as a tris-chelated dication (Figure 7), even though certain counterion in the precursor salts have high coordinating power and the solvent mixture is not strongly ionizing. As in most other similar investigation, the metal-ligand exchange mechanism was not addressed in this investigation.

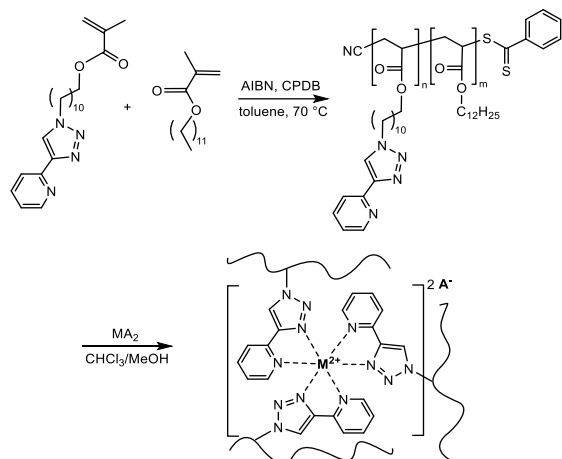


Figure 7. Synthesis of poly(lauryl methacrylate) chains functionalized with bidentate triazole-pyridine ligands, and crosslinking with metal salts.^[29]

Yet another ligand using in self-healing metallopolymers is bipyridine, incorporated within polydimethylsiloxane linear chains (bpy-DMS), which were crosslinked by lanthanide metal cations (Eu^{3+} , Tb^{3+}) from salts with different anions (nitrate, triflate, Figure 8), as well as by $\text{Zn}(\text{OTf})_2$ and $\text{Fe}(\text{OTf})_2$.^[30] This polymer, even prior to metal salt addition, is self-organized with separate domains of π -stacked bpy ligand aggregates in the flexible polymer matrix. This organization is maintained after salt addition, with minor variations of the spacing between the ligand aggregates, as shown by a SAXS study. The Ln^{3+} -ligand interaction in the polymer has a 1:2 stoichiometry, thus the ion coordination is filled with the counterions and/or solvent molecules. The introduction of the Eu^{3+} and Tb^{3+} nitrate salts does not alter the mechanical properties, relative to the metal-free polymer, indicating ineffective crosslinking, whereas improved stretchability and self-healing properties resulted after addition of the triflate salts. The dynamics in these polymers was attributed, however, to the disaggregation of the π -stacked microdomains rather than to ligand exchange processes.

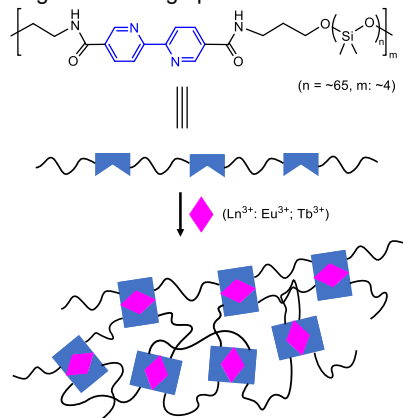


Figure 8. Structure of the bpy-PDMS linear chains and their crosslinking with different metal salts.^[30]

4. Anionic Ligands

4.1. Catechol and other Polyphenol Ligands

Catechol is a weak acid ($\text{pK}_a = 9.45, 12.8$), but the driving force associated to its chelation favors double deprotonation to yield a rather strong complexation of the catecholate dianion (cat^{2-}). The coordination of catechol with Fe^{3+} yields the tris-chelate $[\text{Fe}(\text{cat})_3]^{3-}$ at $\text{pH} > 9.5$, a 1:2 complex at $\text{pH} 6-7$, and the monoadduct at $\text{pH} < 5$.^[31] The self-healing and adhesive behavior in mussel byssal thread, already mentioned above in the neutral histidine ligand section, may also be due to the interaction of the catechol-functionalized dopamine (3,4-dihydroxyphenylalanine, DOPA H_2), which is abundant in mussel byssus proteins, with Fe^{3+} .^[32] On the basis of this hypothesis, various self-healing polymers containing dynamic metal-catechol bonds have been designed and prepared.^[33] It is to be noted that the catechol motif is also increasingly being used to fabricate MOFs.^[34]

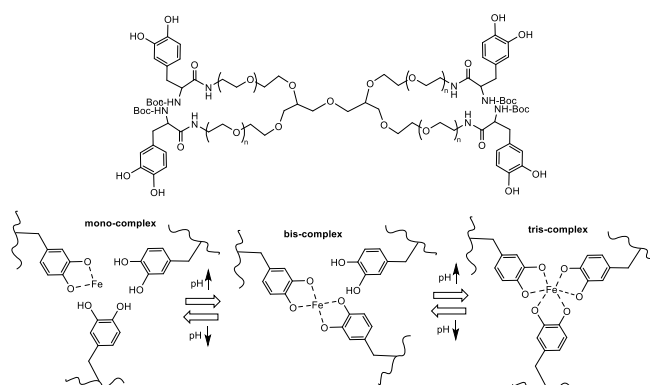


Figure 9. Synthesis of a Fe^{3+} -PEG-dopa $_4$ self-healing material.^[9b]

In the pioneering contribution, a chain-end DOPA H_2 -modified 4-arm star poly(ethylene glycol), Figure 9a, was interacted with FeCl_3 in water with a DOPA $\text{H}_2/\text{Fe}^{3+}$ ratio of 3:1. The Fe^{3+} catechol binding is pH-dependent, turning from green at pH 5 (mono-complex) to blue at pH 8 (bis-complex) and finally red at pH 12 (tris-complex), Figure 9b, and the pH increase induced gelation, to yield an elastic self-healing material.^[9b] Similar materials based on Fe^{3+} -catechol crosslinking have subsequently been reported.^[35] On the basis of a DFT study on the tris(catechol) model complex, $[\text{Fe}(\text{cat})_3]^{3-}$, the exchange was proposed to involve a stepwise chelate opening and full ligand dissociation assisted by external water molecules through H-bonding.^[36]

Self-healing materials with metal-catechol crosslinks have also been developed with ions other than Fe^{3+} . A poly(dopamine acrylamide-*co*-*n*-butyl acrylate) (P(DA-*co*-BA)) copolymer (Figure 10) was crosslinked with Ca^{2+} and Mg^{2+} in different ratios and the self-healing efficiency was studied in sea water, in air and in deionized water. The use of triethylamine prevented the oxidation of the catechol functions under basic conditions. Both Ca^{2+} and Mg^{2+} derivatives showed self-healing in air, water, and seawater at room temperature when only 20% of the catechol functions are

coordinated to the metal complex, whereas no self-healing occurred when the metal content was greater (50% or more). The authors proposed a dissociative exchange for the metal-catechol interactions, with assistance by the H-bonds with water, since self-healing is more efficient in water than in air.

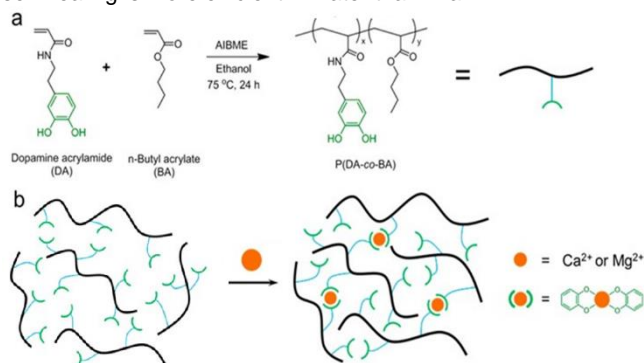


Figure 10. Synthesis of P(DA-co-BA) (a) and crosslinking by Ca^{2+} and Mg^{2+} . Reproduced with permission from ref. [37]. Copyright 2016 American Chemical Society.

4.2. Thiolates.

Coordination adaptable networks with a vitrimer-like behavior were synthesized from a 1:1 mixture of ZnCl_2 and PETMP (pentaerythritol tetrakis(3-mercaptopropionate) ligands), in the presence of a variable amount of TEA to partially deprotonate the PETMP thiol functions, see Figure 11a.[38] The resulting materials were named $\text{PETMP}_{x-y}\text{-Zn}$ (where x and y represent the percentages of protonated and deprotonated thiol ligands, respectively). Hot-pressing of the fully deprotonated $\text{PETMP}_{0-100}\text{-Zn}$ powder was unsuccessful, even at a high temperature of $180\text{ }^\circ\text{C}$. Conversely, with no deprotonation at all, the resulting $\text{PETMP}_{100-0}\text{-Zn}$ sample was a viscous fluid without any mechanical strength. However, materials synthesized from partial deprotonation afforded transparent and reprocessable materials. The lesser the added TEA, the softer the polymer and the lower the reprocessing temperature. The most investigated $\text{PETMP}_{80-20}\text{-Zn}$ material could be reprocessed at $150\text{ }^\circ\text{C}$ and 3 MPa within 10 min. It showed negligible swelling and dissolution in common solvents except DMSO and DMF, where it swelled and became opaque, though the insoluble fraction in these solvents was not reported. On the other hand, the materials completely dissolved at $40\text{ }^\circ\text{C}$ when treated with an excess amount of a thiol (e.g. *p*-methoxybenzenethiol). An Arrhenius behavior was observed for the relaxation time, with a greater E_a for a greater degree of Zn-S bonding (115 kJ/mol for $\text{PETMP}_{80-20}\text{-Zn}$, 121 kJ/mol for $\text{PETMP}_{76-24}\text{-Zn}$). DFT calculations carried out on a $[\text{Zn}(\text{SMe})_4]^{2-}$ molecular model of the network crosslink gave a much lower barrier (33.3 kJ mol⁻¹) for a ligand dissociation assisted by H-bonding to an external thiol function, to yield $[\text{Zn}(\text{SMe})_3]^- + (\text{MeS}\cdots\text{H}\cdots\text{SMe})^-$ (Figure 11b), than for the dissociation without thiol assistance to yield $[\text{Zn}(\text{SMe})_3]^- + \text{MeS}^-$ (68.4 kJ mol⁻¹), leading the authors to suggest a ligand mediated dissociative mechanism. It is to be noted, however, that the chosen molecular model may not be the most appropriate one for the crosslinks in the $\text{PETMP}_{x-y}\text{-Zn}$ materials, which are neutral and presumably also contain residual Zn-Cl bonds. Thus, a dissociative mechanism would entail an energetically costly charge separation to generate a positively charged Zn center. In

addition, as already pointed out above, tricoordination is quite rare for Zn^{2+} .

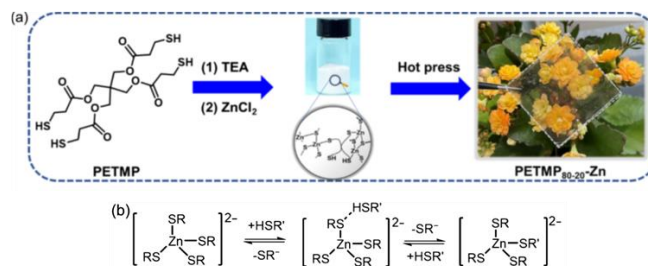


Figure 11. (a) Schematic representation of the Zn^{2+} -crosslinked PETMP ligand network. (b) Proposed ligand mediated dissociative mechanism. Reproduced from ref. [38] with the authors' permission.

4.3. Carboxylates.

Carboxylate ligands are widely used in coordination chemistry, including for the fabrications of a large variety of MOFs, and in biological systems. Due to the presence of two lone pairs on each oxygen atom, different modes of metal-carboxylate interactions are possible, as shown in Figure 12. It is relatively easy to install carboxylic acid functionalities on small molecules and monomers. Hence, these ligands are particularly suitable for the fabrication of CooANs.

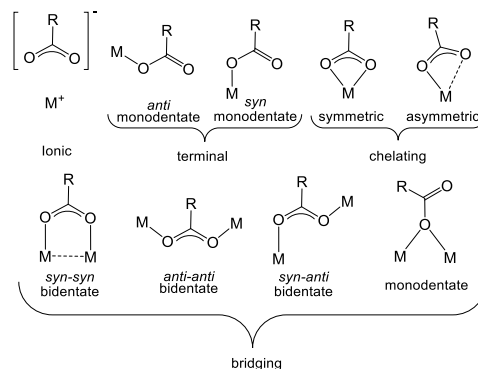


Figure 12. Carboxylate binding modes in metal complexes.

A carboxylic acid-functionalized linear poly(dimethylsiloxane) (PDMS-COOH), containing on average one carboxylic acid for every two-siloxane groups, was crosslinked using ZnCl_2 to yield PDMS-COO-Zn (Figure 13), which behaves as a thermoset at room temperature, but can be reshaped at high temperatures.[39] The metal nature is crucial to afford self-healing properties, because using Fe^{3+} and Cu^{2+} led to non-moldable solid powders at high temperatures, whereas Na^+ led to the formation of liquid-like gels. On the basis on the FTIR spectrum, the crosslink structure was proposed to consist of a tetrahedral Zn coordination geometry with four *syn-syn* bidentate bridging carboxylate ligands. The observed viscosity change with temperature led the authors to propose a dissociative exchange with charge separation, although this is one of those clear examples where such dissociation should be rendered difficult by the low permittivity of the organic matrix and the absence of potentially donor solvents. The presence of residual carboxylic acid functions in the polymer

matrix, as suggested by the FTIR analysis (though these were not quantified by the authors) hints at a more likely associative exchange.

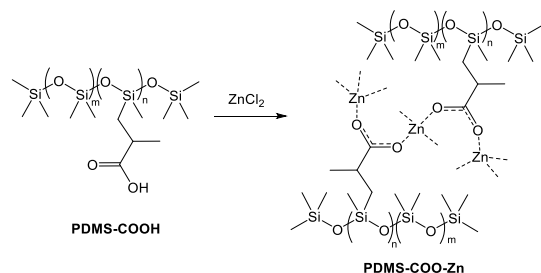


Figure 13. Synthesis of a Zn^{2+} -crosslinked carboxylic acid-functionalized poly(dimethylsiloxane).^[39]

A Zn^{2+} -crosslinked CooAN was also obtained by addition of $\text{Zn}(\text{OAc})_2$ to a COOH-functionalized waterborne polyurethane (WPU), made by the co-condensation of 2,2-bis(hydroxymethyl)propionic acid (DMPA) and a long-chain hydroxy-telechelic poly(tetrahydrofuran) (PTMG, degree of polymerization ca. 2000) with a diisocyanate (IPDI), as shown in Figure 14a. The crosslinks in the final product (WPU-V) are much more dispersed than in the PDMS-COO-Zn material of Figure 13 and were proposed to adopt a bis-chelated mononuclear structure (Figure 14b).^[40] An additional Zn^{2+} -crosslinked carboxylate CooAN, presented in the same contribution, was generated from a polymer obtained by grafting maleic anhydride monomers onto high-density polyethylene chains, to yield an anhydride-functionalized polyethylene called HDPE-M (Figure 14c). In this case, the crosslinks in the final product HDPE-V were proposed to consist of mononuclear bis(carboxylate)-bis(carboxylic acid) complexes. It has to be pointed out, however, that all these structural assignments were based solely on the infrared spectroscopic characterization. For the WPU-V material, even though using a zinc molar amount corresponding to 100% of the polymer-linked carboxylic acids, the gel fraction was only 58.92% in THF at 60 °C. This was rationalized by the strong hydrogen bonding between the chains, which may prevent a more quantitative crosslinking. For the HDPE-V material, given the lack of quantitative determination of the maleic anhydride incorporation in the HDPE chains, the precise Zn/COOH stoichiometry is not known and the obtained HDPE-V crosslinked product showed a gel fraction of 72.03% in toluene at 90°C. Both WPU-V and HDPE-V materials were shown to be reprocessable and the stress relaxation data of WPU-V were shown to follow the Arrhenius law with an activation energy of 87.26 kJmol^{-1} , thus the authors suggested these materials to be coordination vitrimers, characterized by an associative ligand exchange. However, no proof of the ligand exchange mechanism was provided in the publication. As argued in the introduction, an Arrhenius behavior for the viscosity data is insufficient to demonstrate an associative mechanism for the crosslink migration.

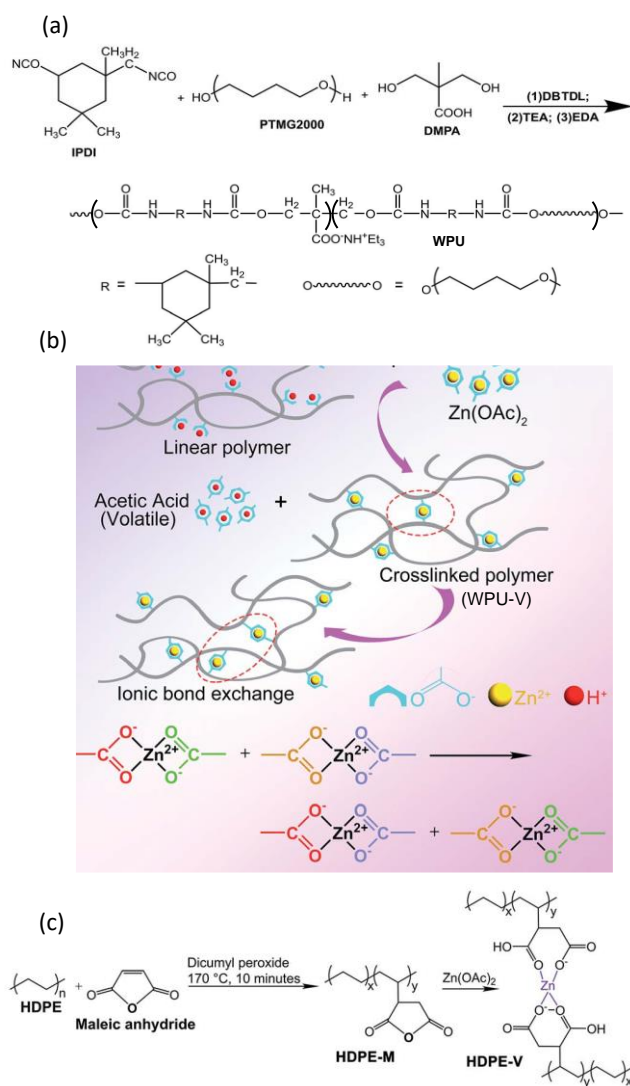


Figure 14. (a) Synthetic scheme for the linear WPU chains. (b) Crosslinking of WPU with $\text{Zn}(\text{OAc})_2$ to produce the WPU-V material. (c) Synthetic scheme for the linear HDPE-M chains and crosslinking to HDPE-V. Reproduced with permission from ref. ^[40]. Copyright 2019 Royal Society of Chemistry.

Linear chains synthesized by random radical copolymerization of 2-ethylhexyl methacrylate with 2-carboxyethyl acrylate (9:1 ratio) were crosslinked with Cu^{2+} using an exchange reaction with $\text{Cu}(\text{OAc})_2 \cdot \text{H}_2\text{O}$ (Figure 15).^[41] The structure of the crosslinking units was assumed to be identical to that of the acetate precursor, namely a paddle wheel dimeric structure with four bridging carboxylate groups. A series of Cu^{2+} -crosslinked copolymers was generated by varying the metal content from 0% to 100%, based on the theoretical coordinating power of the polymer carboxylate groups. The 100% material did not show any self-healing behavior, whereas the samples with 70% substitution or less are malleable at 80 °C. Addition of acetic acid, HCl, water or aqueous ammonia in THF caused complete dissolution, due to exchange reactions with release of the crosslinking interactions. The self-healing of these materials clearly demonstrates the presence of dynamic ligand exchange, but detailed studies on the exchange mechanism were not carried in this investigation.

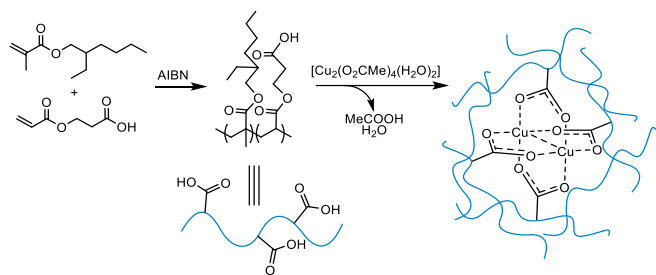


Figure 15. Synthesis of a carboxylic acid-functionalized poly(2-ethylhexyl methacrylate) and crosslinking by exchange with $\text{Cu}(\text{OAc})_2 \cdot \text{H}_2\text{O}$.^[41]

The main group Al^{3+} ion has also been used as a crosslinking metal in combination with carboxylate ligands. The polymer matrix used in this case consisted of carboxyl modified polydimethylsiloxanes linear chains (CPDMS, Figure 16), produced by co-condensation of octamethylcyclotetrasiloxane (D_4) and tetramethyltetra vinylcyclotetrasiloxane (D_4^{VI}), plus 1,3-divinyl-1,1,3,3-tetramethyldisiloxane (MM^{VI}) as a capping agent, to yield a vinyl-functionalized polysiloxane intermediate (PVMS). The dangling carboxylic acid functions were then introduced by a thiol-ene reaction between the vinyl groups and 3-mercaptopropionic acid. The crosslinking was realized under strictly anhydrous conditions using AlCl_3 in a chloroform-acetonitrile mixture.^[42] A series of materials, named $\text{Al}_z\text{-CPDMS}_{x\text{K}-y\text{K}}$, was synthesized by varying the molecular weight ($y\text{K} = 10\text{-}40\text{K}$), the carboxyl grafting density ($x\text{K} =$ average chain length between two grafted carboxyl groups, in the 2-4K range) and the Al^{3+} loading ($z = \text{COOH}/\text{Al}$ molar ratio, from 1 to 6). The mechanical and self-healing properties of the resulting elastic solids could be regulated through the x , y and z parameters. The carboxylate coordination to Al^{3+} was proposed to be monodentate on the basis of FTIR evidence. The free carboxyl absorption band completely disappeared only for $\text{Al}_1\text{-CPDMS}_{2\text{K}-10\text{K}}$, indicating the reluctance of the carboxylic acid functions to replace all chloride ligands in AlCl_3 , even when $\text{COOH}/\text{Al} > 3$. It is to be noted that the crosslinking was carried out without any base to trap the HCl by-product. Here also, the crosslink exchange mechanism was not investigated.

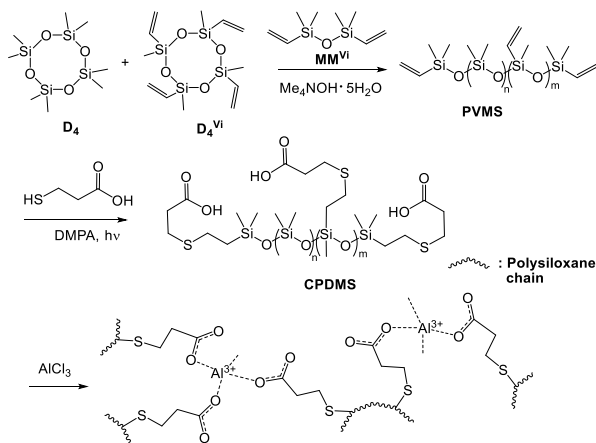


Figure 16. Al^{3+} -crosslinked carboxyl modified polydimethylsiloxanes (CPDMS) networks.^[42]

Carboxylate-functionalized linear polymers have also been crosslinked with a Cu_{12} cuboctahedral cluster (a member of the family of metal-organic polyhedra or MOP), which spontaneously assembles by combination of Cu^{2+} and isophthalic acid (IPA), see Figure 17a.^[43] Linear polymer chains with randomly grafted IPA ligands were first produced by radical polymerization of *n*-butyl acrylate and an acrylate-bearing IPA comonomer (named “acrylic IPA”, Figure 17b), then the addition of copper acetate produced the self-assembled crosslinked network (named MOP-CN), which showed the characteristic temperature-dependent viscosity behavior of vitrimers and could be hot-press reprocessed at 150 °C eight times without altering the mechanical properties. In addition, to the interesting mechanical properties and reprocessability, the MOP cages maintain their microporosity, leading the authors to suggest possible applications in the fabrication of recyclable gas separation membranes. For comparison, a permanent covalent network (PCN) and a weak coordination network (WCN) with the same crosslink density were synthesized by replacing, in the first case, the copper complex with a covalent crosslinker and, in the second case, the acrylic IPA comonomer with simple acrylic acid. The mechanical properties and solvent resistance of MOP-CN are similar to those of PCN, whereas WCN irreversibly elongated upon strain increase. The presence of ligand exchange on the MOP surface had been previously proven by the authors *via* an independent study on molecular models.^[44] A Small Angle Neutron Scattering (SANS) study and an elegant kinetic monitoring by size exclusion chromatography (SEC) of the ligand exchange between a small-size C_{18} -IPA and a large-size PS-MOP (R_1 in Figure 17a = $\text{C}_{18}\text{H}_{37}$ or high-molecular weight polystyrene (PS, 3.3 kg mol⁻¹), see Figure 17c, established that the MOP framework was maintained during the thermally activated ligand exchange and led the authors to propose an associative ligand exchange mechanism.

A final example of a carboxylate-based CooAN, developed in our own lab, is based on a $[\text{Zr}_6\text{O}_4(\text{OH})_4]^{12+}$ cluster as a crosslink. Molecular $[\text{Zr}_6\text{O}_4(\text{OH})_4(\text{O}_2\text{CR})_{12}]_n$ clusters can adopt three possible ligand arrangements (two for $n = 1$ and one for $n = 2$), all featuring a cuboidal arrangement of the $[\text{Zr}_6\text{O}_4(\text{OH})_4]^{12+}$ core with a central octahedral Zr_6 moiety, depending on the carboxylate substituent and crystallization conditions, see Figure 18. The fully symmetric O_h structure has only *syn-syn*-bidentate bridging ligands, the C_{3v} structure has nine *syn-syn*-bidentate bridging and three chelating ligands, and the C_{2h} -symmetric Zr_{12} structure features seven intracluster *syn-syn*-bidentate bridging ligands (six “belt-bridging”, spanning an edge between the outer and the inner triangular faces, and one “inner-face-bridging”, spanning an edge of the inner face) and three chelating ligands for each Zr_6 cluster, plus four *syn,anti*-bridging ligands (two per Zr_6 unit), which connect the two clusters to each other. Previous work has also shown that, depending on conditions, some or all the carboxylate ligands can be exchanged with free carboxylic acids.^[45]

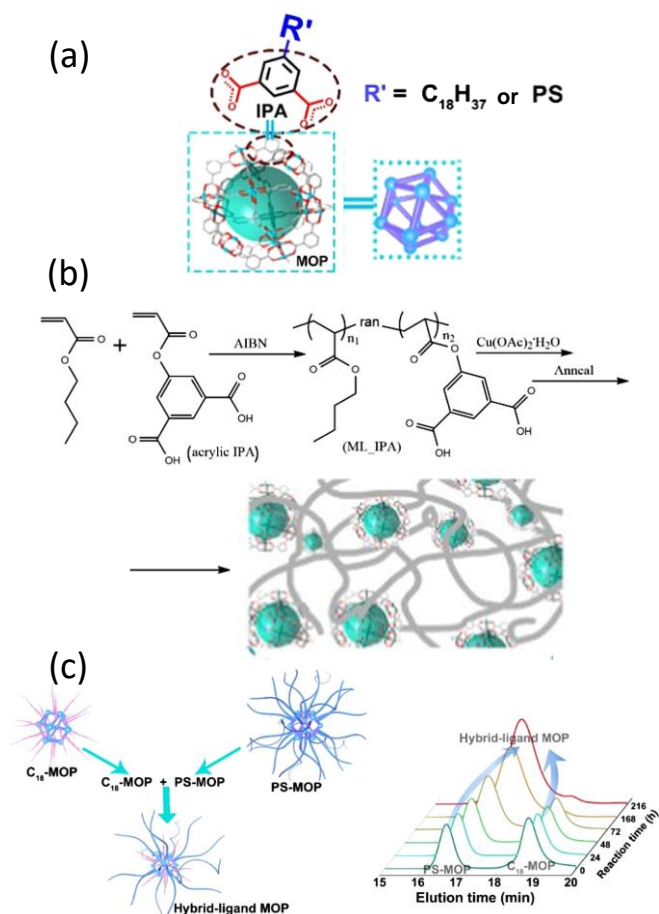


Figure 17. (a) Topology of the $\text{Cu}_{12}(\text{IPA})_{12}$ MOP. (b) Preparation of MOP crosslinked network (MOP-CN). (c) Ligand exchange between C_{18} -IPA and PS-MOP, with monitoring by Size Exclusion Chromatography. Reproduced from ref. [43] with the authors' permission.

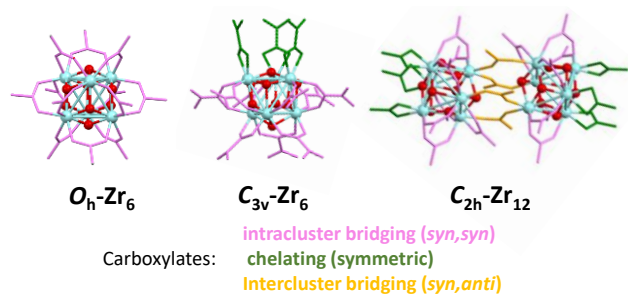
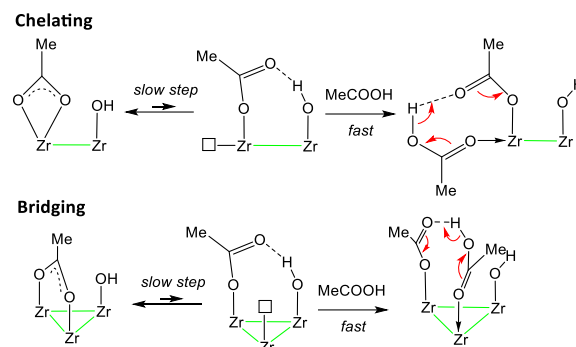


Figure 18. Topology of the $[\text{Zr}_6\text{O}_4(\text{OH})_4(\text{O}_2\text{CR})_{12}]_n$ clusters ($n = 1$ or 2).

$[\text{Zr}_6\text{O}_4(\text{OH})_4]$ -crosslinked CooANs with different COOH/Zr_6 ratios, exhibiting vitrimer-like properties,^[46] were made by carboxylate-ligand exchange from $[\text{Zr}_6\text{O}_4(\text{OH})_4(\text{O}_2\text{CMe})_{12}]_2$ and a COOH -functionalized polymethacrylate (the same polymer shown in Figure 15a). Parallel investigations with flexible molecular linkers (adipic acid, sebacic acid) revealed the incorporation of only up to eight carboxylates per Zr_6 cluster, which parallels the stoichiometry of certain $[\text{Zr}_6\text{O}_4(\text{OH})_4]$ -based MOFs, namely $[\text{Zr}_6\text{O}_4(\text{OH})_8(\text{H}_2\text{O})_4(\text{O}_2\text{CR})_8]$.^[47] The percent of polymer-linked COOH groups exchanged by the cluster was therefore based on this stoichiometry. The prepared $[\text{Zr}_6\text{O}_4(\text{OH})_4]$ -based CooANs

(named Zr-CooAN-x , where x is the percent of polymer COOH functions linked to the Zr_6 clusters) were flexible and reshapable 3D materials with x up to 50, whereas Zr-CooAN-100 is brittle and could not be reshaped by hot-pressing. The conditions needed to hot-press reshape the Zr-CooAN-x materials were milder for lower x : 100°C for $x = 50$, 75°C for $x = 25$ and 20 , 50°C for $x = 15$, 10 and 5 . All mechanical and rheological properties of Zr-CooAN-10 were essentially identical before and after reshaping.



Scheme 4. Operationally associative exchange with a rate-determining partial dissociation, assisted by a neighboring OH ligand, for chelating and bridging acetates in compound $[\text{Zr}_6\text{O}_4(\text{OH})_8(\text{H}_2\text{O})_4(\text{O}_2\text{CR})_8]$.^[48]

The question of the carboxylate exchange mechanism in these Zr-CooAN-x materials has attracted our keen attention, because classification as a “coordination vitrimer” requires proof that the crosslink migration follows an associative mechanism. Further drive was given by the lack of absolute proof (from the kinetic-mechanistic point of view) of an associative migration for any of the other CooANs outlined in this review, and by the scarcity of kinetic-mechanistic investigations of the carboxylate/carboxylic acid exchange in molecular complexes. It is important to point out that the conditions leading to the synthesis and reshaping of the Zr-CooAN-x materials are such that the all three possible structures shown in Figure 18 can exist and interconvert, hence the carboxylate ligands may be bonded to the $[\text{Zr}_6\text{O}_4(\text{OH})_4]$ core in all possible modes. Variable-temperature and variable-ratio ^1H NMR studies, in combination with DFT calculations, were carried out for the exchange of acetates with free acetic acid in the model C_{2h} -symmetric $[\text{Zr}_6\text{O}_4(\text{OH})_4(\text{O}_2\text{CMe})_{12}]_2$ compound.^[48] The results indicate that both chelating and belt-bridging acetates exchange rapidly (resonance coalescence on the NMR timescale) with a rate-determining partial dissociation (zero order in free CH_3COOH), assisted by the cluster triply bridging hydroxide ligand ($\mu_3\text{-OH}$) to yield an H-bonded intermediate, followed by rapid associative scrambling (Scheme 4). Hence, the exchange processes are operationally associative. The inner-face-bridging and intercluster-bridging acetates, on the other hand, do not yield any observable exchange up to 70°C . The exchange processes are enthalpically driven, being faster for the chelating acetates ($\Delta H^\ddagger = 15.0 \pm 0.4$ kcal mol^{-1} ; $\Delta S^\ddagger = 8 \pm 1$ cal $\text{mol}^{-1} \text{K}^{-1}$) and slower for the belt-bridging ones ($\Delta H^\ddagger = 20.6\text{-}22.7$ kcal mol^{-1} ; $\Delta S^\ddagger = 9\text{-}13$ cal $\text{mol}^{-1} \text{K}^{-1}$) because of the greater release of steric strain in the chelate binding mode. Hence, this model investigation fully supports the classification of the Zr-CooAN-x materials as “coordination vitrimers”.

5. Conclusion

The research area of Coordination Adaptable Networks, of rather recent development, is currently burgeoning. The available array of metal ions, metal ion clusters and exchangeable ligands, in combination with the variability and tuneability of ligand-functionalized polymers - in terms of (co)monomers, average chain length and dispersity, density of grafted ligand and architecture – makes the engineering of CooANs limited only by our imagination. Work published so far in this area has only scratched the surface. The rheological properties of the fabricated materials also sharply depend on the ligand/metal ratio. Relative to the more intensely investigated CAN analogues, CooANs present distinct features such as moldability under (generally) milder conditions and the presence of specific properties associated to the metals (optical, magnetic, etc.). Metal complexation to ligand-functionalized polymers has also been used as a reinforcement in other covalent adaptable networks.

As illustrated by the critical analysis of several examples in this review, the material moldability is intimately associated to the nature of the metal-ligand interactions, while the rheological behavior is modulated by the chemical constitution of the polymer matrix. Full understanding of both polymer physical chemistry and coordination chemistry is thus required to design materials with targeted properties.

Vitrimer-like moldability (*i.e.* a viscosity following the Arrhenius law) is ensured by the associative nature of the ligand exchange process responsible for the crosslink migration, although certain dissociative networks also exhibit this behavior. Therefore, the intimate mechanism of the migration process cannot be proven solely on the basis of the viscosity analysis; mechanistic investigations on suitable model coordination compounds are of great help. Profound knowledge of coordination chemistry is thus essential. In particular, proper consideration must be given to the potential coordinating properties of the anions introduced with the metal crosslinker, to the possible presence of other coordinating additives (*e.g.* moisture) and to the permittivity of the medium (*e.g.* dry or swollen) in which reshaping occurs.

6. Acknowledgements

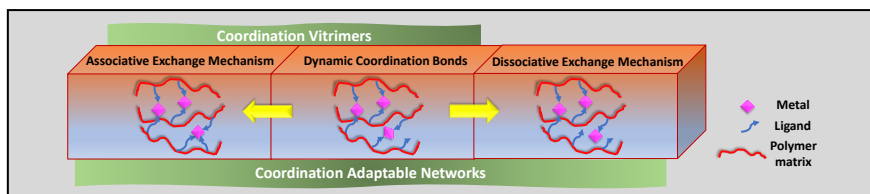
We are grateful to the French National Research Agency (AFRCAN program, ANR-19-CE06-0014) for funding.

Keywords: Coordination adaptable networks • Reshapable polymer materials • Associative ligand exchange • Dissociative ligand exchange • Vitrimers

- [1] S. V. Wanasinghe, O. J. Dodo, D. Konkolewicz, *Angew. Chem. Int. Ed.* **2022**, *61*.
- [2] a) R. H. Colby, J. R. Gillmor, M. Rubinstein, *Phys. Rev. E* **1993**, *48*, 3712-3716; b) M. Rubinstein, A. N. Semenov, *Macromolecules* **1998**, *31*, 1386-1397; c) F. Tanaka, *Polymer Physics: Applications to Molecular Association and Thermoreversible Gelation*, Cambridge University Press, Cambridge, **2011**, p.
- [3] a) X. X. Chen, M. A. Dam, K. Ono, A. Mal, H. B. Shen, S. R. Nutt, K. Sheran, F. Wudl, *Science* **2002**, *295*, 1698-1702; b) Y. Zhang, A. A. Broekhuis, F. Picchioni, *Macromolecules* **2009**, *42*, 1906-1912; c) P. Reutenauer, E. Buhler, P. J. Boul, S. J. Candau, J. M. Lehn, *Chem. Eur. J.* **2009**, *15*, 1893-1900; d) C. J. Kloxin, T. F. Scott, B. J. Adzima, C. N. Bowman, *Macromolecules* **2010**, *43*, 2643-2653.
- [4] a) T. F. Scott, A. D. Schneider, W. D. Cook, C. N. Bowman, *Science* **2005**, *308*, 1615-1617; b) R. Nicolay, J. Kamada, A. Van Wassen, K. Matyjaszewski, *Macromolecules* **2010**, *43*, 4355-4361; c) Y. Amamoto, H. Otsuka, A. Takahara, K. Matyjaszewski, *Adv. Mater.* **2012**, *24*, 3975-3980.
- [5] D. Montarnal, M. Capelot, F. Tournilhac, L. Leibler, *Science* **2011**, *334*, 965-968.
- [6] W. Denissen, J. M. Winne, F. E. Du Prez, *Chem. Sci.* **2016**, *7*, 30-38.
- [7] A. Jourdain, R. Asbai, A. Omaima, M. M. Chehimi, E. Drockenmuller, D. Montarnal, *Macromolecules* **2020**, *53*, 1884-1900.
- [8] O. J. L., H. M. T., L. Carolina, F. J. Gabriel, M.-G. N., V. Margarita, A.-P. Julia, d. I. R. J. Antonio, I. I. A., R. A. Peralta, *Coord. Chem. Rev.* **2023**, *496*, 215403.
- [9] a) M. Burnworth, L. Tang, J. R. Kumpfer, A. J. Duncan, F. L. Beyer, G. L. Fiore, S. J. Rowan, C. Weder, *Nature* **2011**, *472*, 334-337; b) N. Holten-Andersen, M. J. Harrington, H. Birkedal, B. P. Lee, P. B. Messersmith, K. Y. C. Lee, J. H. Waite, *Proc. Nat. Acad. Sci.* **2011**, *108*, 2651-2655.
- [10] a) B. Sandmann, S. Bode, M. D. Hager, U. S. Schubert in *Metallopolymers as an Emerging Class of Self-Healing Materials*, Vol. 262 (Ed. V. Percec), **2013**, pp. 239-257; b) M. Enke, D. Dohler, S. Bode, W. H. Binder, M. D. Hager, U. S. Schubert in *Intrinsic Self-Healing Polymers Based on Supramolecular Interactions: State of the Art and Future Directions*, Vol. 273 Eds.: M. D. Hager, S. VanDerZwaag and U. S. Schubert), **2016**, pp. 59-112; c) H. Li, P. Yang, P. Pageni, C. B. Tang, *Macromol. Rapid Comm.* **2017**, *38*; d) G. I. Dzhardimatieva, B. C. Yadav, S. Singh, I. E. Uflyand, *Dalton Trans.* **2020**, *49*, 3042-3087; e) C.-H. Li, J.-L. Zuo, *Adv. Mater.* **2020**, *32*, 1903762; f) S. Basak, A. Bandyopadhyay, *J. Organomet. Chem.* **2021**, *956*; g) S. Gotz, S. Zechel, M. D. Hager, G. R. Newkome, U. S. Schubert, *Progr. Polym. Sci.* **2021**, *119*, 101428.
- [11] R. Hajj, A. Duval, S. Dhers, L. Avérous, *Macromolecules* **2020**, *53*, 3796-3805.
- [12] S. Wang, S. Q. Ma, O. Li, X. W. Xu, B. B. Wang, K. F. Huang, Y. L. Liu, J. Zhu, *Macromolecules* **2020**, *53*, 2919-2931.
- [13] S. K. Schoustra, M. M. J. Smulders, *Macromol. Rapid Comm.*
- [14] R. J. Sundberg, R. B. Martin, *Chem. Rev.* **1974**, *74*, 471-517.
- [15] S. Zechel, M. D. Hager, T. Priemel, M. J. Harrington, *Biomimetics* **2019**, *4*, 20.
- [16] D. Mozhdehi, S. Ayala, O. R. Cromwell, Z. Guan, *J. Am. Chem. Soc.* **2014**, *136*, 16128-16131.
- [17] D. Mozhdehi, J. A. Neal, S. C. Grindy, Y. Cordeau, S. Ayala, N. Holten-Andersen, Z. Guan, *Macromolecules* **2016**, *49*, 6310-6321.
- [18] M. Enke, R. K. Bose, S. Zechel, J. Vitz, R. Deubler, S. J. Garcia, S. van der Zwaag, F. H. Schacher, M. D. Hager, U. S. Schubert, *Polym. Chem.* **2018**, *9*, 3543-3551.
- [19] Y. Marcus, *Chem. Rev.* **1988**, *88*, 1475-1498.
- [20] D. K. Coggin, J. A. Gonzalez, A. M. Kook, D. M. Stanbury, L. J. Wilson, *Inorg. Chem.* **1991**, *30*, 1115-1125.
- [21] G. Anantharaman, K. Elango, *Organometallics* **2007**, *26*, 1089-1092.
- [22] a) M. J. Harrington, J. H. Waite, *J. Experim. Biol.* **2007**, *210*, 4307-4318; b) D. E. Fullenkamp, L. He, D. G. Barrett, W. R. Burghardt, P. B. Messersmith, *Macromolecules* **2013**, *46*, 1167-1174; c) M. Enke, S. Bode, J. Vitz, F. H. Schacher, M. J. Harrington, M. D. Hager, U. S. Schubert, *Polymer* **2015**, *69*, 274-282; d) S. C. Grindy, R. Learsch, D. Mozhdehi, J. Cheng, D. G. Barrett, Z. B. Guan, P. B. Messersmith, N. Holten-Andersen, *Nat. Mater.* **2015**, *14*, 1210-1216; e) M. Enke, F. Jehle, S. Bode, J. Vitz, M. J. Harrington, M. D. Hager, U. S. Schubert, *Macromol. Chem. Phys.* **2017**, *218*, 1600458; f) J. Ahner, D. Pretzel, M. Enke, R. Geitner, S. Zechel, J. Popp, U. S. Schubert, M. D. Hager, *Chem. Mater.* **2018**, *30*, 2791-2799; g) A. Trapaidze, M. D'Antuono, P. Fratzi, M. J. Harrington, *Eur. Polym. J.* **2018**, *109*, 229-236.
- [23] a) S. Tang, B. D. Olsen, *Macromolecules* **2016**, *49*, 9163-9175; b) T. T. H. Pham, J. van der Gucht, J. M. Kleijn, M. A. C. Stuart, *Soft Matter* **2016**, *12*, 4979-4984; c) S. C. Grindy, M. Lenz, N. Holten-Andersen, *Macromolecules* **2016**, *49*, 8306-8312; d) S. C. Grindy, N. Holten-Andersen, *Soft Matter* **2017**, *13*, 4057-4065; e) Q. Tang, D. L. Zhao, Q. Zhou, H. Y. Yang, K. Peng, X. Y. Zhang, *Macromol. Rapid Comm.* **2018**,

- 39, 1800109; f) Q. Tang, D. L. Zhao, H. Y. Yang, L. J. Wang, X. Y. Zhang, *J. Mater. Chem. B* **2019**, *7*, 30-42.
- [24] S. V. Wegner, F. C. Schenk, S. Witzel, F. Bialas, J. P. Spatz, *Macromolecules* **2016**, *49*, 4229-4235.
- [25] S. Bode, L. Zedler, F. H. Schacher, B. Dietzek, M. Schmitt, J. Popp, M. D. Hager, U. S. Schubert, *Adv. Mater.* **2013**, *25*, 1634-1638.
- [26] S. Bode, R. K. Bose, S. Matthes, M. Ehrhardt, A. Seifert, F. H. Schacher, R. M. Paulus, S. Stumpf, B. Sandmann, J. Vitz, A. Winter, S. Hoepfener, S. J. Garcia, S. Spange, S. van der Zwaag, M. D. Hager, U. S. Schubert, *Polym. Chem.* **2013**, *4*, 4966-4973.
- [27] S. Kupfer, L. Zedler, J. Guthmuller, S. Bode, M. D. Hager, U. S. Schubert, J. Popp, S. Grafe, B. Dietzek, *Phys. Chem. Chem. Phys.* **2014**, *16*, 12422-12432.
- [28] S. Bode, M. Enke, R. K. Bose, F. H. Schacher, S. J. Garcia, S. van der Zwaag, M. D. Hager, U. S. Schubert, *J. Mater. Chem. A* **2015**, *3*, 22145-22153.
- [29] B. Sandmann, B. Happ, S. Kupfer, F. H. Schacher, M. D. Hager, U. S. Schubert, *Macromol. Rapid Comm.* **2015**, *36*, 604-609.
- [30] Y. L. Rao, V. Feig, X. D. Gu, G. J. N. Wang, Z. A. Bao, *J. Polym. Sci., Polym. Chem.* **2017**, *55*, 3110-3116.
- [31] a) M. J. Sever, J. J. Wilker, *Dalton Trans.* **2004**, 1061-1072; b) J. T. Weisser, M. J. Nilges, M. J. Sever, J. J. Wilker, *Inorg. Chem.* **2006**, *45*, 7736-7747.
- [32] J. Yu, W. Wei, E. Danner, R. K. Ashley, J. N. Israelachvili, J. H. Waite, *Nature Chemical Biology* **2011**, *7*, 588-590.
- [33] a) A. Andersen, Y. Chen, H. Birkedal, *Biomimetics* **2019**, *4*, 30; b) H. Birkedal, Y. Q. Chen in *Mussel inspired self-healing materials: Coordination chemistry of polyphenols*, Vol. 76 Eds.: D. RuizMolina and R. VanEldik, **2020**, pp. 269-298.
- [34] a) B. F. Abrahams, J. Coleiro, K. Ha, B. F. Hoskins, S. D. Orchard, R. Robson, *J. Chem. Soc., Dalton Trans.* **2002**, 1586-1594; b) K. Nakabayashi, S. Ohkoshi, *Inorg. Chem.* **2009**, *48*, 8647-8649; c) S. Morikawa, T. Yamada, H. Kitagawa, *Chem. Lett.* **2009**, *38*, 654-655; d) B. F. Abrahams, T. A. Hudson, L. J. McCormick, R. Robson, *Crystal Growth & Design* **2011**, *11*, 2717-2720; e) M. Hmadeh, Z. Lu, Z. Liu, F. Gandara, H. Furukawa, S. Wan, V. Augustyn, R. Chang, L. Liao, F. Zhou, E. Perre, V. Ozolins, K. Suenaga, X. F. Duan, B. Dunn, Y. Yamamoto, O. Terasaki, O. M. Yaghi, *Chem. Mater.* **2012**, *24*, 3511-3513; f) N. T. T. Nguyen, H. Furukawa, F. Gándara, C. A. Trickett, H. M. Jeong, K. E. Cordova, O. M. Yaghi, *J. Am. Chem. Soc.* **2015**, *137*, 15394-15397.
- [35] a) H. Ceylan, M. Urel, T. S. Erkal, A. B. Tekinay, A. Dana, M. O. Guler, *Adv. Funct. Mater.* **2013**, *23*, 2081-2090; b) M. Krogsgaard, M. A. Behrens, J. S. Pedersen, H. Birkedal, *Biomacromolecules* **2013**, *14*, 297-301; c) P. S. Yavvari, A. Srivastava, *J. Mater. Chem. B* **2015**, *3*, 899-910; d) P. Sun, J. Wang, X. Yao, Y. Peng, X. Tu, P. Du, Z. Zheng, X. Wang, *ACS Appl. Mater. Interf.* **2014**, *6*, 12495-12504; e) B. J. Kim, D. X. Oh, S. Kim, J. H. Seo, D. S. Hwang, A. Masic, D. K. Han, H. J. Cha, *Biomacromolecules* **2014**, *15*, 1579-1585; f) N. N. Xia, X. M. Xiong, J. H. Wang, M. Z. Rong, M. Q. Zhang, *Chem. Sci.* **2016**, *7*, 2736-2742; g) W. C. Huang, F. Ali, J. S. Zhao, K. Rhee, C. C. Mou, C. J. Bettinger, *Biomacromolecules* **2017**, *18*, 1162-1171; h) Z. W. Tang, M. C. Zhao, Y. Wang, W. L. Zhang, M. Zhang, H. Xiao, L. L. Huang, L. H. Chen, X. H. Ouyang, H. B. Zeng, H. Wu, *Int. J. Biol. Macromol.* **2020**, *144*, 127-134; i) X. Q. Jin, H. H. Jiang, Z. M. Zhang, Y. J. Yao, X. J. Bao, Q. L. Hu, *Carbohydr. Polym.* **2021**, *254*; j) F. Wang, Z. Yang, J. Li, C. Zhang, P. Sun, *ACS Macro Lett.* **2021**, *10*, 510-517; k) M. X. Li, M. Z. Rong, M. Q. Zhang, *Express Polym. Lett.* **2021**, *15*, 781-790; l) M. Paolieri, Z. Chen, F. Babu Kadumudi, M. Alehosseini, M. Zorrón, A. Dolatshahi-Pirouz, H. Maleki, *ACS Appl. Nano Mater.* **2023**, *6*, 5211-5223; m) Y.-J. Zhu, S.-C. Huang, Z.-G. Qian, X.-X. Xia, *Biomacromolecules* **2023**, *24*, 1774-1783.
- [36] Q. Liu, X. Lu, L. Li, H. Zhang, G. Y. Liu, H. Zhong, H. B. Zeng, *J. Phys. Chem. C* **2016**, *120*, 21670-21677.
- [37] J. Li, H. Ejima, N. Yoshie, *ACS Appl. Mater. Interf.* **2016**, *8*, 19047-19053.
- [38] W. Li, H.-Q. Wang, W.-T. Gao, Z. Wang, P. Xu, H. Ma, C.-H. Li, *CCS Chem.* **2022**, *4*, 3781-3797.
- [39] J. C. Lai, L. Li, D. P. Wang, M. H. Zhang, S. R. Mo, X. Wang, K. Y. Zeng, C. H. Li, Q. Jiang, X. Z. You, J. L. Zuo, *Nat. Commun.* **2018**, *9*, 2725.
- [40] Y. Wang, Z. Liu, C. Zhou, Y. Yuan, L. Jiang, B. Wu, J. Lei, *J. Mater. Chem. A* **2019**, *7*, 3577-3582.
- [41] Y. Vidavsky, S. Bae, M. N. Silberstein, *J. Polym. Sci., Polym. Chem.* **2018**, *56*, 1117-1122.
- [42] Y. Lei, W. Huang, Q. Huang, A. Zhang, *New J. Chem.* **2019**, *43*, 261-268.
- [43] M. Zhang, H. Yu, Q. Zou, Z.-A. Li, Y. Lai, L. Cai, P. Yin, *CCS Chem.* **2022**, *4*, 3563-3572.
- [44] M. Zhang, S. He, Q. Zou, Z.-A. Li, Y. Lai, K. Chen, L. Ma, J.-F. Yin, M. Li, C. He, Y. Ke, P. Yin, *J. Phys. Chem. Lett.* **2021**, *12*, 5395-5403.
- [45] a) M. Puchberger, F. R. Kogler, M. Jupa, S. Gross, H. Fric, G. Kickelbick, U. Schubert, *Eur. J. Inorg. Chem.* **2006**, 3283-3293; b) P. Walther, M. Puchberger, F. R. Kogler, K. Schwarz, U. Schubert, *Phys. Chem. Chem. Phys.* **2009**, *11*, 3640-3647; c) J. Kreutzer, M. Czakler, M. Puchberger, E. Pittenauer, U. Schubert, *Eur. J. Inorg. Chem.* **2015**, 2889-2894; d) J. Kreutzer, M. Puchberger, C. Artner, U. Schubert, *Eur. J. Inorg. Chem.* **2015**, 2145-2151.
- [46] M. Murali, D. Berne, C. Joly-Duhamel, S. Caillol, E. Leclerc, E. Manoury, V. Ladmiral, R. Poli, *Chem. Eur. J.* **2022**, *28*, e202202058.
- [47] a) W. Morris, B. Voloskiy, S. Demir, F. Gandara, P. L. McGrier, H. Furukawa, D. Cascio, J. F. Stoddart, O. M. Yaghi, *Inorg. Chem.* **2012**, *51*, 6443-6445; b) J. E. Mondloch, W. Bury, D. Fairen-Jimenez, S. Kwon, E. J. DeMarco, M. H. Weston, A. A. Sarjeant, S. T. Nguyen, P. C. Stair, R. Q. Snurr, O. K. Farha, J. T. Hupp, *J. Am. Chem. Soc.* **2013**, *135*, 10294-10297; c) M. Lammert, H. Reinsch, C. A. Murray, M. T. Wharmby, H. Terraschke, N. Stock, *Dalton Trans.* **2016**, *45*, 18822-18826.
- [48] M. Murali, C. Bijani, J.-C. Daran, E. Manoury, R. Poli, *Chem. Sci.* **2023**, *14*, 8152-8163.

Entry for the Table of Contents



Known Coordination Adaptable Networks (CooANs) have been classified by type of exchanging ligands; special attention has been devoted to the mechanism of ligand exchange responsible for crosslink migration, possibly allowing them to be considered as “coordination vitrimers”.

Institute and/or researcher Twitter usernames: @LCC_CNRS